J|A|C|S
ARTICLES
Published on Web 02/04/2006

Molecular Recognition between Protein and Nicotinamide Dinucleotide in Intact, Proton-Translocating Transhydrogenase Studied by ATR-FTIR Spectroscopy

Masayo Iwaki,[‡] Nick P. J. Cotton,[†] Philip G. Quirk,[†] Peter R. Rich,[‡] and J. Baz Jackson*[,†]

Contribution from the School of Biosciences, University of Birmingham, Edgbaston Birmingham B15 2TT, UK, and Department of Biology, University College London, Gower Street, London, WC1E 6BT, UK

Received August 17, 2005; E-mail: j.b.jackson@bham.ac.uk

Abstract: Nicotinamide dinucleotide binding to transhydrogenase purified from *Escherichia coli* was investigated by attenuated total reflectance-Fourier transform infrared (ATR-FTIR) spectroscopy. Detergent-free transhydrogenase was deposited as a thin film on an ATR prism, and spectra were recorded during perfusion with buffers in the presence and absence of dinucleotide ($NADP^+$, NADPH, NAD^+, or NADH) in both H_2O and D_2O media. IR spectral changes were attributable to the bound dinucleotides and to changes in the protein itself. The dissociation constant of NADPH was estimated to be approximately 5 μM from a titration of the magnitude of the IR changes against the nucleotide concentration. IR spectra of related model compounds were used to assign principle bands of the dinucleotides. This information was combined with IR data on amino acids and with protein crystallographic data to identify interactions between specific parts of the dinucleotides and their binding sites in the protein. Several IR bands of bound nucleotide were sharpened and/or shifted relative to those in aqueous solution, reflecting a restriction to motion and a change in environment upon binding. Alterations in the protein secondary structure indicated by amide I/II changes were distinctly different for NADP(H) and for NAD(H) binding. The data suggest that NADP(H) binding leads to perturbation of a deeply buried part of the polypeptide backbone and to protonation of a carboxylic acid residue.

Introduction

Transhydrogenase is located in the inner membrane of mitochondria and in the cytoplasmic membrane of bacteria (for reviews see refs 1−3). It couples the transfer of a hydride ion equivalent between NAD(H) and NADP(H) to translocation of protons across the membrane (Scheme 1).

The enzyme normally operates from left to right, driven by the proton electrochemical gradient generated by the respiratory (or sometimes photosynthetic) electron transport chain. Transhydrogenase has three structural components, designated dI, dII, and dIII. The dI component, which binds NAD(H), and the dIII component, which binds NADP(H), protrude from the membrane toward the matrix in mitochondria and toward the cytoplasm in bacteria (Figure 1). The dII component spans the membrane. Transhydrogenase from *Escherichia coli* is composed of two subunits, α and β.[4] The α subunit contains all of dI and the N-terminal region of dII, and the β subunit contains the C-terminal region of dII and all of dIII. The intact enzyme is thought to be an $\alpha_2\beta_2$ tetramer. High-resolution structures of dI and dIII from several species and of a dI_2dIII_1 complex from *Rhodospirillum rubrum* have led to descriptions of the nucleotide-binding sites and to a clear indication as to how the dihydronicotinamide ring of NADH and the nicotinamide ring of $NADP^+$ are brought into apposition at the interface between dI and dIII to effect hydride transfer.[5−9] This site is probably more than 30 Å from the proton translocation pathway in dII, and it has been suggested that proton translocation is linked to hydride transfer by conformational changes that are transmitted between dII and dIII. X-ray and NMR studies have revealed some structural details of likely catalytic reaction intermediates,[10] but important details of the coupling mechanism remain unresolved.

Scheme 1. Chemical Reaction in Transhydrogenase

$$NADH + NADP^+ + H^+_{out} \leftrightarrow NAD^+ + NADPH + H^+_{in}$$

[†] University of Birmingham.
[‡] University College London.

(1) Jackson, J. B. *FEBS Lett.* **2003**, *545*, 18−24.
(2) Jackson, J. B.; White, S. A.; Quirk, P. G.; Venning, J. D. *Biochemisry* **2002**, *41*, 4173−4185.
(3) Jackson, J. B.; White, S. A.; Brondijk, T. H. C. In *Biophysical and Structural Aspects of Bioenergetics*; Wikström, M., Ed.; Royal Society of Chemistry: Cambridge, 2005; Chapter 16, pp 376−393.
(4) Clarke, D. M.; Bragg, P. D. *Eur. J. Biochem.* **1985**, *149*, 517−523.
(5) Buckley, P. A.; Jackson, J. B.; Schnieder, T.; White, A. A.; Rice, D. W.; Baker, P. J. *Structure* **2000**, *8*, 809−815.
(6) Prasad, G. S.; Wahlberg, M.; Sridhar, V.; Sundaresan, V.; Yamaguchi, M.; Hatefi, Y.; Stout, C. D. *Biochemistry* **2002**, *41*, 12745−12754.
(7) Prasad, G. S.; Sridhar, V.; Yamaguchi, M.; Hatefi, Y.; Stout, C. D. *Nat. Struct. Biol.* **1999**, *6*, 1126−1131.
(8) White, S. A.; Peake, S. J.; McSweeney, S.; Leonard, G.; Cotton, N. P. J.; Jackson, J. B. *Structure* **2000**, *8*, 1−12.
(9) Cotton, N. P. J.; White, S. A.; Peake, S. J.; McSweeney, S.; Jackson, J. B. *Structure* **2001**, *9*, 165−176.

10.1021/ja0556272 CCC: $33.50

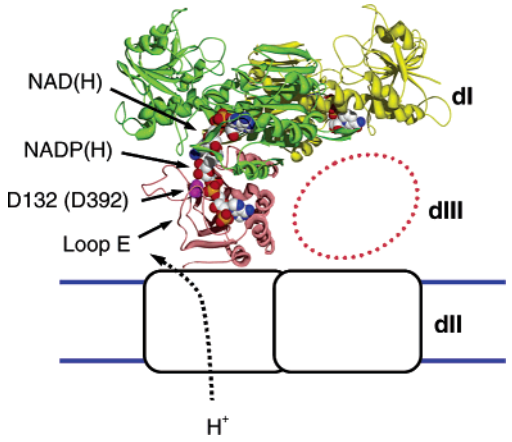

Figure 1. A cartoon representing the structure of transhydrogenase. The ribbons correspond to the three polypeptides of the dI_2dIII_1 complex of *R. rubrum* transhydrogenase (dI in green and in yellow, dIII in red).[10] The probable, approximate positions of the second dIII (red oval) and the two dII components (black rectangles) are shown relative to the membrane (blue lines). Nucleotides, in standard atom colors, and the invariant Asp132 (βAsp392 in *E. coli* transhydrogenase), in purple, are shown in space-filling format.

Fourier transform infrared (FTIR) difference spectroscopy has become a useful technique to investigate structural changes in substrates, cofactors, and amino acid residues within proteins.[11,12] Measurements in the attenuated total reflection (ATR) mode[13−16] are particularly powerful in the case of some membrane proteins: films of membrane proteins may be deposited on the ATR prism, and IR changes may be then recorded during perfusion with different buffers.[17,18] This technique has been used to study the structural changes that accompany ligand binding,[19,20] redox reactions,[21] and the formation of reaction intermediates[22,23] in a range of enzymes. In the present paper, ATR-FTIR spectroscopy has been used to investigate molecular changes induced by dinucleotide binding to intact transhydrogenase from *E. coli*.

Results

NAD(P)(H)-Induced ATR-FTIR Difference Spectra of Transhydrogenase. A thin film of detergent-depleted transhydrogenase was deposited onto the surface of a silicon ATR prism. After rehydration and perfusion for 1 h with nucleotide-free buffer, the absorbance of the protein amide II band at 1545 cm^{-1} stabilized typically at around 0.15−0.18 (see Supporting Information) during subsequent perfusion. Dinucleotide-induced difference spectra were obtained from data collected as nucleotide-free and nucleotide-containing buffer were alternately perfused over the sample (Figure 2). These difference spectra were reversible over many cycles (typically 100 cycles were repeated over 24 h) so that data could be averaged. Figure 2 shows averaged difference spectra for the four nucleotides, NAD^+, NADH, $NADP^+$, and NADPH. The spectral features marked in Figure 2 and described below were reproducible in films made from at least two different protein preparations.

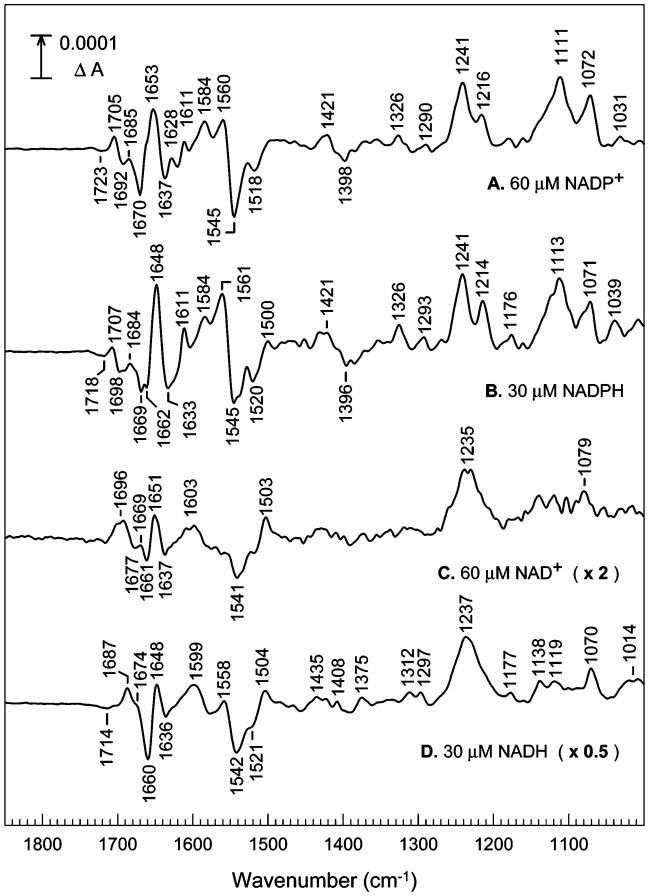

Figure 2. Dinucleotide-induced ATR-FTIR difference spectra of transhydrogenase in H_2O media. The perfusion buffer was 0.1 M potassium phosphate, 2 mM $MgCl_2$, pH 7.2 with and without $NADP^+$ (A, 60 μM), NADPH (B, 30 μM), NAD^+ (C, 60 μM), and NADH (D, 30 μM). Spectra are, respectively, averages of 50, 70, 40, and 40 cycles.

The low concentrations of free nucleotides in the perfusion buffers (<100 μM) were too small to make a significant, direct contribution to the spectra of Figure 2. Only the bound nucleotides that concentrated within the protein binding sites (estimated to be the order of 0.5−1 mM), together with changes occurring in the protein itself, were observable. The positive features in these IR difference spectra can, in principle, arise either from bound ligand or from changes in the protein, whereas the negative features can only arise from changes in the protein. The $NADP^+$- and NADPH-induced difference spectra had features in common, as did the NAD^+- and NADH-induced difference spectra. However, there were distinctive differences between the NADP(H) spectra, on one hand, and the NAD(H) spectra, on the other. Shared features in the $NADP^+$/NADPH difference spectra were observed at 1705/1707(+), 1692/1698(−), 1685/1684(+), 1670/1669(−), 1653/1648(+),

(10) Mather, O. C.; Singh, A.; van Boxel, G. I.; White, S. A.; Jackson, J. B. *Biochemistry* **2004**, *43*, 10952−10964.
(11) Mäntele, W. *Biophysical Techniques in Photosynthesis*; Amesz, J., Hoff, A. J., Eds.; Kluwer Academic Publishers: Dordrecht, 1996; pp 137−160.
(12) Barth, A.; Zscherp, C. *Q. Rev. Biophys.* **2002**, *35*, 369−430.
(13) Goormaghtigh, E.; Raussens, V.; Ruysschaert, J.-M. *Biochim. Biophys. Acta* **1999**, *1422*, 105−185.
(14) Heberle, J.; Zscherp, C. *Appl. Spectrosc.* **1996**, *50*, 588−596.
(15) Tatulian, S. A. *Biochemistry* **2003**, *42*, 11898−11907.
(16) Marrero, H.; Rothschild, K. J. *Biophys. J.* **1987**, *52*, 629−635.
(17) Rich, P. R.; Iwaki, M. In *Biophysical and Structural Aspects of Bioenergetics*; Wikström, M., Ed.; Royal Society of Chemistry; Cambridge, 2005; Chapter 13, pp 314−333.
(18) Nyquist, R. M.; Heitbrink, D.; Bolwien, C.; Wells, T. A.; Gennis, R.; Heberle, J. *FEBS Lett.* **2001**, *505*, 63−67.
(19) Ryan, S. E.; Hill, D. G.; Baenziger, J. E. *J. Biol. Chem.* **2002**, *277*, 10420−10426.
(20) Iwaki, M.; Rich, P. R. *J. Am. Chem. Soc.* **2004**, *126*, 2386−2389.
(21) Iwaki, M.; Osyczka, A.; Moser, C. C.; Dutton, P. L.; Rich, P. R. *Biochemistry* **2004**, *43*, 9477−9486.
(22) Iwaki, M.; Puustinen, A.; Wikström, M.; Rich, P. R. *Biochemistry* **2003**, *42*, 8809−8817.
(23) Nyquist, R. M.; Heitbrink, D.; Bolwien, C.; Gennis, R. B.; Heberle, J. *Proc. Natl. Acad. Sci. U.S.A.* **2003**, *100*, 8715−8720.

1637/1633(−), 1611/1611(+), 1584/1584(+), 1560/1561(+), 1545/1545(−), 1518/1520(−), 1421/1421(+), 1398/1396(−), 1326/1326(+), 1290/1293(+), 1241/1241(+), 1216/1214(+), 1111/1113(+), 1072/1071(+), and 1031/1039(+) cm^{-1}. Shared features in the NAD^+/NADH-difference spectra were observed at 1696/1687(+), 1661/1660(−), 1651/1648(+), 1637/1636(−), 1603/1599(+), 1541/1542(−), 1503/1504(+), 1235/1237(+), and 1079/1070(+) cm^{-1}. A positive band was observed at 1628 cm^{-1} in the $NADP^+$-induced spectrum but not in the NADPH spectrum; a negative band was observed at 1662 cm^{-1} in the NADPH spectrum but not in the $NADP^+$ spectrum. A shared feature in the difference spectra of both NADPH and NADH was seen at 1176/1177(+) cm^{-1}. Note that because the affinity of transhydrogenase for NAD^+ is rather weak[24] (see below), ligand binding in the experiment shown in Figure 2C was incomplete and the changes in the spectrum were relatively small (the scale is expanded ×2). Consequently some of the features in the NAD^+-induced difference spectrum were more difficult to resolve than those in the other spectra.

Effects of H/D Exchange. The effect of substituting a D_2O-based buffer system on the absolute ATR-FTIR spectrum of a transhydrogenase film is shown in the Supporting Information. The amide II band was downshifted by ∼100 cm^{-1} in the D_2O buffer, and the extent of loss of the 1545 cm^{-1} peak indicated that H/D exchange in the protein was >90% complete. To aid band assignments, difference spectra induced by $NADP^+$, NADPH, and NADH were also measured in D_2O media (the affinity for NAD^+ was too low to provide spectra of adequate signal/noise). In all three dinucleotide-induced difference spectra, small downshifts were observed in the 1706−1610 cm^{-1} region, in D_2O relative to H_2O, as expected for amide I bands,[13,25] and upshifts in the bands, between 1241 and 1214 cm^{-1} (Figure 3). In the case of NADP(H)-difference spectra, several components of the amide II changes were downshifted to 1434/1433 and/or 1476/1477 cm^{-1} upon H/D exchange (as expected for amide II bands) but the prominent trough at 1545 cm^{-1} remained with a small upshift ($\Delta\nu = +2-4$ cm^{-1}). In contrast, the NADH-induced difference spectrum in D_2O showed the expected downshift of all features in the amide II region, with the trough at 1542/1521 cm^{-1} downshifting to 1456/1439 cm^{-1}.

IR Spectra of NAD(P)(H) and Related Model Compounds in Solution. Absolute spectra of the free forms of NAD(P)(H) are shown in Figure 4. These spectra are useful in the assignment of positive bands in the dinucleotide-induced difference spectra (Figures 2 and 3). However, available information to aid assignment of the nucleotide IR bands to specific chemical groups within NAD(P)(H) is limited. Therefore, the IR spectra of a range of model materials related to fragments of the ligands were also recorded (Figure 5). A simple comparison of the absolute spectra, combined with available literature information,[26−30] has allowed assignments of the majority of bands in the dinucleotide-induced spectra to specific fragments of the ligands and, in some cases, to the principle bonds involved.

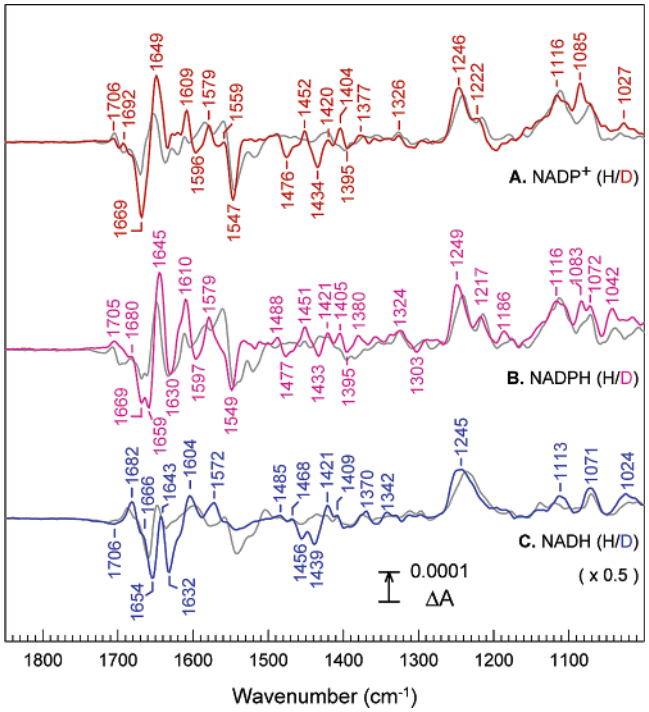

Figure 3. Dinucleotide-induced ATR-FTIR difference spectra in transhydrogenase in D_2O media. The perfusion buffer was 0.1 M potassium phosphate, 2 mM $MgCl_2$, pD 7.2 with and without $NADP^+$ (A, 60 μM, red), NADPH (B, 30 μM, pink), and NADH (C, 30 μM, blue). Spectra are averages of 10 cycles. Data in H_2O media (taken from Figure 2A, B, and D) are overlaid in gray for comparison.

Ribose does not absorb significantly in the 1800−1200 cm^{-1} window of the IR spectrum (Figure 5B). Hence, all the major bands in the adenosine spectrum above 1200 cm^{-1} (Figure 5C) must arise from the adenine ring system (Figure 5A). It is clear, therefore, that the bands at 1650 (in part), 1606, 1579−81, 1481, 1421−3 (in part), 1380, 1336−9, and 1304−6 cm^{-1} in the solution spectra of NAD(P)(H) (Figure 4) must also arise from the adenine moiety of the dinucleotides: they are equivalent to the bands in the solution spectra of adenosine (and related materials) at 1650, 1604, 1580, 1481, 1424, 1378, 1336, and 1304 cm^{-1}. It is also clear from a comparison of the adenine-containing models of Figure 5A/C and D/F that the broad band at 1236−8 cm^{-1} in the NAD(P)(H) spectra can be assigned to the P−O stretch of the pyrophosphate bridge that links the nicotinamide and adenosine moieties.

The broad overlapping bands around 1100 cm^{-1} are dominated by P−O groups and are particularly strong in the NADP(H) spectra because of the additional 2′-phosphate on the adenine ribose.[28,29] Also present in this region, but masked by the phosphate bands, are the weaker contributions from ribose OH bonds.[27] These are evident in the 1120−1045 cm^{-1} region of the solution spectra of adenosine, ADP, and ADP-ribose.

The nicotinamide mononucleotides, NMN^+ and NMNH (Figure 5H,J), are particularly informative as to the major contributions from the nicotinamide and dihydronicotinamide moieties to the NAD(P)(H) spectra of Figure 4. Hence, the redox-sensitive bands at 1696 and 1688 cm^{-1} may be assigned to the carboxamide carbonyl stretch[26] of the nicotinamide and the dihydronicotinamide rings, respectively. A band at 1545/

(24) Bizouarn, T.; van Boxel, G. I.; Bhakta, T.; Jackson, J. B. *Biochim. Biophys. Acta* **2005**, *1708*, 404−410.
(25) Haris, P. I.; Lee, D. C.; Chapman, D. *Biochim. Biophys. Acta* **1986**, *874*, 255−265.
(26) İde, S.; Ataç, A.; Yurdakal, S. *J. Mol. Struct.* **2002**, *605*, 103−107.
(27) Benedetti, E.; Bramanti, E.; Papineschi, F.; Rossi, I.; Benedetti, E. *Appl. Spectrosc.* **1997**, *51*, 792−797.
(28) Barth, A.; Mäntele, W. *Biophys. J.* **1998**, *75*, 538−544.
(29) Takeuchi, H.; Murata, H.; Harada, I. *J. Am. Chem. Soc.* **1988**, *110*, 392−397.
(30) Chen, D.; Yue, K. T.; Martin, C.; Rhee, K. W.; Sloan, D.; Callender, R. *Biochemistry* **1987**, *26*, 4776−4784.

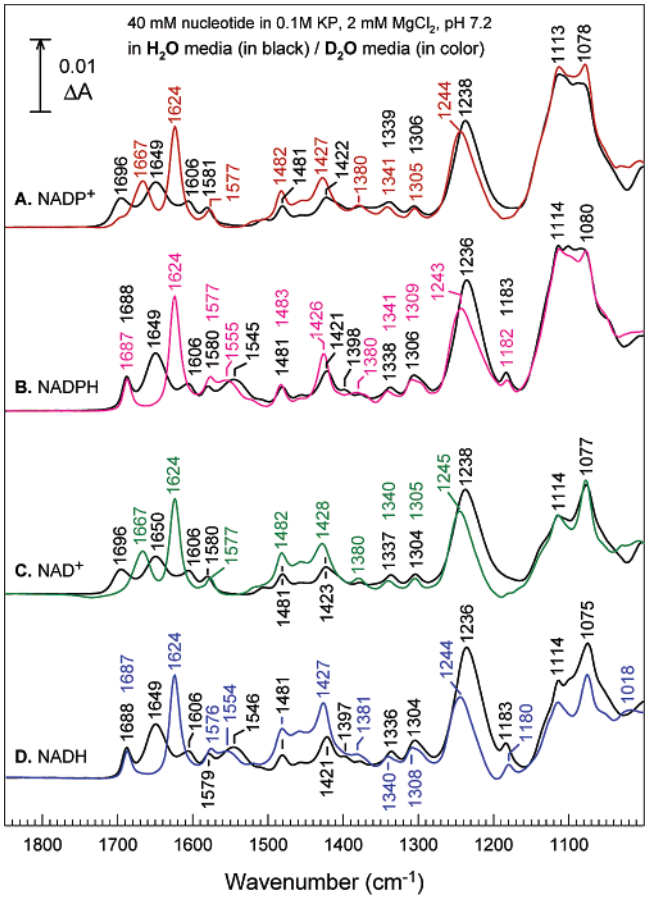

Figure 4. Absolute ATR-FTIR spectra of $NADP^+$, NADPH, NAD^+, and NADH in H_2O (black) and in D_2O (color) media. All nucleotides were 40 mM in 0.1 M potassium phosphate, 2 mM $MgCl_2$, pH/D 7.2. Buffer contributions have been subtracted from the spectra shown.

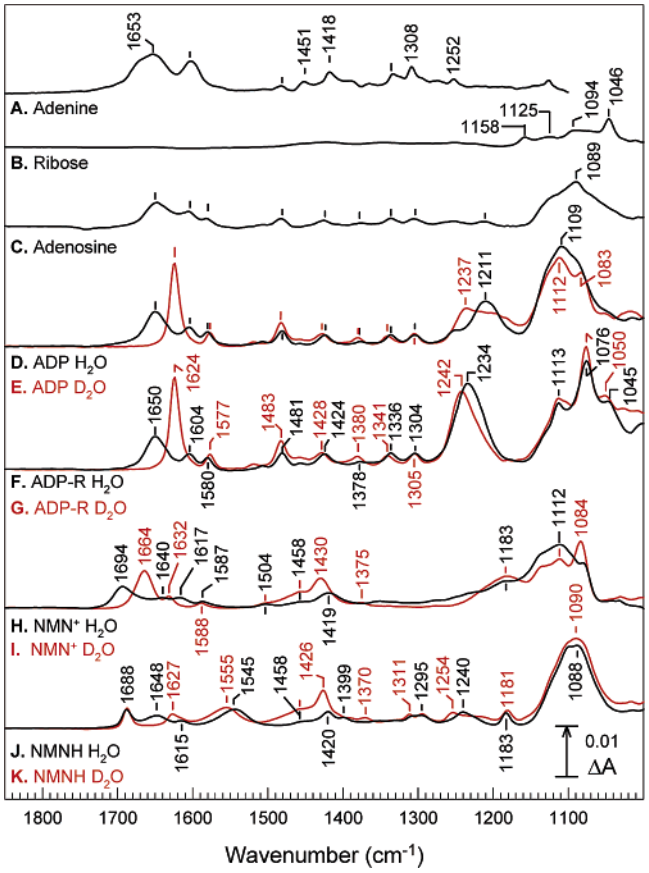

Figure 5. Absolute ATR-FTIR spectra of model compounds related to NAD(P)(H). The adenine was measured in 96% ethanol. Spectra of ribose, adenosine, adenosine diphosphate (ADP), adenosine 5′ diphospho ribose (ADP-R), and oxidized and reduced forms of nicotinamide mononucleotide (NMN^+ and NMNH), all at 40 mM, were measured in H_2O and in D_2O media (0.1 M potassium phosphate, 2 mM $MgCl_2$, pH/D 7.2). Spectra of solvents and buffers have been subtracted from the spectra shown. In traces A, C, and D, peak positions that are identical to the ones in trace F are indicated by short bars without labeling.

1546 cm^{-1} is found in the NAD(P)H but not in the $NAD(P)^+$ spectra, and it is equivalent to the band found at 1545 cm^{-1} in NMNH but not in NMN^+. It probably corresponds to the stretching frequency of the C−N bond within the substituent carboxamide group at the 3-position of the dihydronicotinamide ring. There are also weak bands at 1397−8 and 1183 cm^{-1} in the NAD(P)H but not in the $NAD(P)^+$ spectra (Figure 4), and these are equivalent to the 1399 and 1183 cm^{-1} bands, respectively, of NMN(H). These features are useful markers for determination of the redox state of the nicotinamide dinucleotides. Some IR bands in the solution spectra of NAD(P)(H), for example, those at 1421−1423 cm^{-1}, may have contributions from both the nicotinamide and adenine moieties. The band at 1649 cm^{-1} in NAD(P)H is probably due mainly to adenine with a small contribution from dihydronicotinamide.

Several large effects of H/D exchange are evident in the NAD(P)(H) spectra (Figure 4), and again, these tend to be mirrored in the ADP, ADP-ribose, and NMN(H) models of Figure 5. Hence, in the spectra of both the reduced and oxidized forms of the dinucleotides, the band at 1649−1650 cm^{-1}, which mainly arises from the adenine moiety, was downshifted by 27−26 cm^{-1} upon H/D exchange. In the oxidized forms of the dinucleotides, the 1696 cm^{-1} band was downshifted by 29 cm^{-1} and increased in intensity when H_2O was replaced with D_2O. Equivalently, the 1699 cm^{-1} band in NMN^+ was downshifted by 30 cm^{-1} in the D_2O buffer. In contrast, in the reduced forms of the dinucleotides and in NMNH, the band at 1688 cm^{-1} was barely affected by H/D exchange, and the band at 1545/1546 cm^{-1} was upshifted by 8−10 cm^{-1}. In all the NADP(H) dinucleotides, the band at 1421−1423 cm^{-1}, which has contributions from both adenine and NMN(H), was upshifted by 5−7 cm^{-1} and increased in intensity. The band at 1238 cm^{-1}, which can be assigned to a phosphate P−O stretch, also showed a clear upshift of 6−8 cm^{-1} in all dinucleotides as well as in ADP-ribose. These shifts were useful in the assignment of bands in the dinucleotide-induced difference spectra of transhydrogenase shown in Figures 2 and 3 (see below). Possible IR band assignments of dinucleotides in solution are summarized in the Supporting Information (Table S1).

Estimation of Nucleotide Binding Constants. NADPH-induced difference spectra were recorded at a range of nucleotide concentrations (see Supporting Information). The shapes of the ATR-FTIR difference spectra were similar for NADPH concentrations between 0.5 and 100 μM. This indicates that the character of the binding reaction detected by the FTIR changes was independent of the nucleotide concentration. The amplitudes of the 1561/1546 cm^{-1} peak/trough and of the peak at 1241 cm^{-1} (see Figure 2) were plotted as a function of the NADPH concentration (Figure 6). Since the nucleotide solution flows continuously over the film during the recording, it can be assumed that binding to the protein reaches an equilibrium in

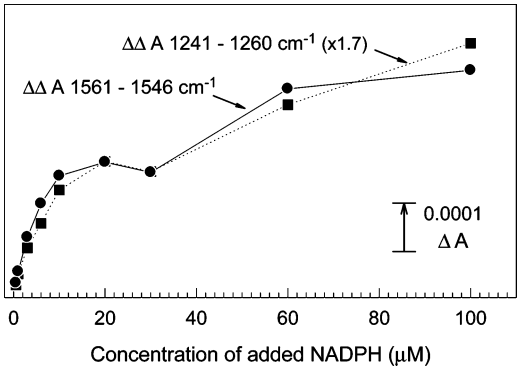

Figure 6. The dependence of FTIR spectral changes on NADPH concentration. Amplitudes of a spectral shift ($\Delta\Delta A$ 1561−1546 cm^{-1}) and a peak ($\Delta\Delta A$ 1241−1260 cm^{-1}) in NADPH-induced difference spectra are plotted against the concentration of NADPH in the perfusion buffer (0.1 M potassium phosphate, 2 mM $MgCl_2$, pH 7.2).

which the concentration of unbound nucleotide is given by that in the perfusant reservoir and that the FTIR absorbance change is proportional to the fractional occupation of the binding sites. In this case, the K_d is given by the concentration of NADPH needed for half saturation. However, both curves showed two phases with apparent dissociation constants of 5 μM and 50 μM. The former is in rough agreement with the $K_d \approx 0.9$ μM determined by microcalorimetry.[24] The difference between the two sets of measurements may arise partly because the FTIR experiments were performed in a detergent-free, wild-type sample, whereas the microcalorimetry experiments were carried out with a detergent-dispersed, cysteine-free enzyme. For the other nucleotides, only a few concentrations were tested in equivalent experiments (not shown), and this established that NADH and $NADP^+$ also bound with K_d values in the range 10^{-5}−10^{-4} M but that NAD^+ bound somewhat more weakly.

Discussion

A central question in the mechanism of action of transhydrogenase is how hydride transfer between dinucleotide substrates is coupled to proton translocation across the membrane. Almost certainly, the coupling involves large conformational changes in the protein, and the consensus view is that these conformational changes are linked to alterations in the binding energies of the dinucleotides.[1,31−33] Changes at the NAD(H) site are probably involved in gating the hydride-transfer reaction.[10] Changes at the NADP(H) site may be involved in switching the proton access of the translocation apparatus; the conformation of this site is opened and occluded during turnover to allow or prevent, respectively, the exchange of NADP(H) with the solvent.[1,3] The sensitivity of IR absorbance changes to protein and ligand conformation suggests that this methodology will be helpful in understanding the mechanism of coupling between hydride transfer and proton translocation. In this report, we have measured IR changes in a film of transhydrogenase deposited on an ATR prism, a technique[17,18] that is ideally suited for use with membrane proteins. The reversibility of the spectral changes during nucleotide binding and the similarity of measured K_d values to those obtained with the detergent-dispersed protein[24] suggest that the integrity of the ligand-binding sites is maintained during the production of the film.

In general, NADP(H)-induced difference spectra showed common features that are different from equivalent NAD(H)-induced spectra. This reflects the different characteristics of NADP(H) binding to the dIII site and NAD(H) binding to the dI site that are also evident in X-ray structures of the isolated components and of the *R. rubrum* dI_2dIII_1 complex.[9] The structural features responsible for differences between NAD(P)$^+$ and NAD(P)H binding have not yet been identified from crystal structures: for example, at 2 Å resolution it is difficult to detect changes in the atomic structure of isolated dIII when bound $NADP^+$ is substituted with NADPH.[10] However, chemical shift changes of amide groups are clearly detectable in NMR experiments after the nucleotide substitution; they extend from the nucleotide-binding site into adjacent loops and helices.[34,35] The FTIR experiments reported here reveal spectral differences between the $NADP^+$- and NADPH-bound states and between the NAD^+- and NADH-bound states of the intact transhydrogenase (Figures 2A/B and 2C/D, respectively).

Interpretation of Binding Spectra. Tentative assignments of features in the dinucleotide-induced difference spectra (Figure 2) can be made by reference to the solution spectra of the dinucleotides (Figure 4) and by comparison with the effects of H/D exchange. It is clear from the analysis that the difference spectra arise from bound forms of the dinucleotides and from structural alterations of the protein itself.

Bands Due to Bound Ligands. The dinucleotide-induced difference spectra of Figure 2 contain a number of positive bands that can be attributed to bound nucleotides on the basis of their correspondence with peaks in the absolute spectra of the free nucleotides in solution (Figure 4). Bound ligand bands are often sharpened, presumably reflecting a restriction to motion of the ligand upon binding, and shifted, indicating a change in the local environment of the nucleotide. Because of the lower affinity for NAD^+,[24] the site occupancy and, therefore, the signal amplitude of the NAD^+-induced spectrum (Figure 2C) are lower than those of the others. Nevertheless, as the peak height at 1235 cm^{-1} is still 3.5 times higher than the expected intensity of the 1238 cm^{-1} band of 60 μM free NAD^+, it can be deduced that even this weak spectrum arises mainly from protein-bound NAD^+.

Pyrophosphate bands at 1250−1210 cm^{-1} are prominent in the four NAD(P)(H)-induced difference spectra (Figure 2). In the NADP(H)-difference spectra, the 2′-phosphate bands below 1120 cm^{-1} are also pronounced. As for the free ligands (Figure 4), the pyrophosphate bands attributable to the bound NAD(P)(H) were upshifted by 3−8 cm^{-1} on H/D exchange (Figure 3). The pyrophosphate bands of both $NADP^+$ and NADPH are split into bands at 1241 and 1216/1214 cm^{-1} when the nucleotide is bound, presumably because of a more restricted set of possible conformations imposed by binding. Crystal structures of transhydrogenase components from other species[7,8] show that Coulombic interactions between equivalents of the invariant residues, βArg350 (−NH_2 group) and βAsp392 (−COOH group), and the NADP(H) pyrophosphate may be

(31) Hutton, M.; Day, J. M.; Bizouarn, T.; Jackson, J. B. *Eur. J. Biochem.* **1994**, *219*, 1041−1051.
(32) Hatefi, Y.; Yamaguchi, M. *FASEB J.* **1996**, *10*, 444−452.
(33) Bizouarn, T.; Fjellström, O.; Meuller, J.; Axelsson, M.; Bergkvist, A.; Johansson, C.; Karlsson, G.; Rydström, J. *Biochim. Biophys. Acta* **2000**, *1457*, 211−218.
(34) Quirk, P. G.; Jeeves, M.; Cotton, N. P. J.; Smith, K. J.; Jackson, J. B. *FEBS Lett.* **1999**, *446*, 127−132.
(35) Bergkvist, A.; Johansson, C.; Johansson, T.; Rydström, J.; Karlsson, B. G. *Biochemistry* **2000**, *39*, 12595−12605.

significant in this binding. The pyrophosphate bands in the NAD(H)-induced difference spectra are broader and similar band splitting is not evident, suggesting that interaction between pyrophosphate and protein in the dI binding site is weaker or more heterogeneous. Crystal structures that show that NAD(H) can adopt different conformations in this site[9] provide some support for this. Interconversion of these conformations is achieved by bond rotation in the pyrophosphate/ribose phosphate regions and is thought to be important in moving the (dihydro)nicotinamide ring into position for hydride transfer at the appropriate step in the proton-translocation cycle.[10]

Additional positive bands of the bound nucleotides must also be present in the difference spectra, though some could overlap with protein components making them difficult to identify. However, it seems clear that the bands at 1176/1177 cm^{-1} in the NADPH- and NADH-induced spectra arise from the redox-sensitive nicotinamide band (at 1183 cm^{-1} in free NAD(P)H) and that the pair of bands in the NADP(H)-induced spectra at 1326 and 1290−1293 cm^{-1} arise from the adenine moiety (1338−1339 and 1306 cm^{-1} in the free dinucleotides). The 1297 cm^{-1} band in the NADH-induced spectrum probably has a similar origin. It also seems likely that at least part of the positive band seen at 1421−35 cm^{-1} in the difference spectra arises from the equivalent nicotinamide and adenine bands of the model materials. Unfortunately, the H/D effect on this band, which was seen clearly in the free nucleotide spectra, is difficult to estimate in the difference spectra since amide II bands move down to overlap this region in the D_2O spectra (Figure 4).

Bands due to NAD(P)(H) above 1500 cm^{-1} in the difference spectra will, in general, be hidden by stronger amide I and II shifts from the protein (discussed below). However, one particularly clear nucleotide vibrational mode is that of the 3-carboxamide carbonyl group of the nicotinamide ring at 1696 cm^{-1} in the solution spectra of free $NAD(P)^+$, and of the same group associated with the dihydronicotinamide ring at 1688 cm^{-1} in the solution spectra of free NAD(P)H. A candidate for this IR signature in the NADP(H)-induced difference spectra could be the peak at 1705−1707 cm^{-1}. However, in the $NAD(P)^+$ solution spectra, H/D exchange causes a 29 cm^{-1} downshift in the 1696 cm^{-1} band (Figure 4), whereas an upshift of 1 cm^{-1} occurs in the 1705 cm^{-1} band of the $NADP^+$-induced difference spectrum (Figure 3). It is concluded, therefore, that the 1705−7 cm^{-1} band does not arise from the ligand but may instead be associated with changes in a carboxylic acid group of an amino acid residue in the protein (discussed below). There are also bands at 1685/1684 cm^{-1} in the NADP(H)-induced difference spectra and at 1696 and 1687 cm^{-1}, respectively, in the NAD^+ and NADH difference spectra (Figure 2) which might be candidates for the nicotinamide-3-carboxamide groups of the bound nucleotides. The 1685 cm^{-1} band is lost from the $NADP^+$-induced difference spectrum, and (like the 1687/1688 cm^{-1} bands in the solution spectra of NAD(P)H) the 1687/1684 cm^{-1} bands remain in the NAD(P)H difference spectra, on H/D exchange (compare Figures 3 and 4). This behavior is consistent with the assignment of these bands to the nicotinamide 3-carboxamide group.

The peaks at 1648−1653 cm^{-1} in NAD(P)(H)-induced difference spectra should contain a contribution from the adenine ring mode of the bound nucleotide. However, the lower H/D sensitivity of these features compared with those of the nucleotide solution spectra suggests that the bands arise predominantly from vibrational modes of the protein. Several other bands in the dinucleotide-induced difference spectra at 1599−1611, 1421−1435, and 1290−1326 cm^{-1} might plausibly correspond to those seen in the solution spectra. A study using isotopically labelled materials could resolve the ligand-derived bands from those originating in the protein.

Bands Due to Amide I/II Shifts. In addition to features arising directly from the bound ligand, the nucleotide-induced difference spectra of Figure 2 also contain signals arising from perturbation of the protein. A change in the intensity of a protein band upon nucleotide binding will give rise either to a positive or to a negative feature in the difference spectrum, and a change in frequency will lead to a peak/trough pair. Importantly, any negative band must arise from a change in protein structure and cannot be directly associated with nucleotide.

In IR difference spectra of proteins, the majority of changes in the 1690−1620 cm^{-1} and 1570−1520 cm^{-1} regions typically arise from amide I (80% C═O stretch) and amide II (60% N—H bending and 40% C—N stretch) due to alterations in protein conformation. The frequencies of individual amide I bands are dependent on the types of secondary structures that they form.[36] In general, the exchange of solvent H_2O for D_2O affects amide I modes weakly ($\Delta\nu \leq -5$ cm^{-1}) and amide II modes more strongly ($\Delta\nu = -80$ to -100 cm^{-1}; see also Supporting Information). The changes in these regions in the ligand-induced difference spectra of transhydrogenase (Figure 2) arise predominantly from changes in the amide I/II bands. This conclusion is supported by the H/D exchange effects (Figure 3), where small downshifts of bands in the amide I region occur together with much larger downshifts in the amide II region. The magnitudes of the amide I/II band changes are, however, not exceptionally large in comparison with amide I/II changes observed in ligand- or redox-induced changes in a number of other proteins.[17] This suggests that they arise from relatively restricted conformational changes, most likely around the substrate-binding sites. An exception would be the strong H/D-insensitive trough at 1545 cm^{-1} in the NADP(H)-binding spectra that must be arise from a buried amide bond that cannot easily undergo H/D exchange (see below). However, it should also be noted that relative movements of rigid domains in the protein would also cause only small amide I/II band changes that would be restricted to hinge regions. The existence of such interdomain movements cannot be addressed with the present data.

The changes occurring in the amide I region in response to NADP(H) binding are very different from those occurring in response to NAD(H) binding. Amide I frequencies around 1650 cm^{-1} are associated with α-helix. Hence, a preliminary interpretation might be that NAD(P)(H) binding induces some rearrangement/conversion to create additional α-helical structure, although the magnitude of the changes indicates that only a small number of bonds is involved. Studies of NADP(H)-binding kinetics and affinities in wild-type and mutant transhydrogenase have previously revealed the central importance of conformational changes in this region of the protein.[31,37−41]

(36) Stuart, B. *Infrared Spectroscopy: Fundamentals and Applications*; John Wiley & Sons: Chichester, 2004.
(37) Diggle, C.; Bizouarn, T.; Cotton, N. P. J.; Jackson, J. B. *Eur. J. Biochem.* **1996**, *241*, 162−170.
(38) Hu, X.; Zhang, J.; Fjellström, O.; Bizouarn, T.; Rydström, J. *Biochemistry* **1999**, *38*, 1652−1658.
(39) Bragg, P. D.; Hou, C. *Arch. Biochem. Biophys.* **1999**, *363*, 182−190.

The NADH-induced difference spectra exhibited typical amide II troughs at 1542/1521 cm^{-1}, which were entirely downshifted to 1456/1439 cm^{-1} upon H/D exchange. On the other hand, a particularly interesting feature in the NADP(H)-binding spectra is the negative band in the amide II region at 1545 cm^{-1}. This was rather insensitive to H/D exchange in contrast to the small amide II trough at 1518/1520 cm^{-1}, which appeared to be characteristically downshifted to 1434/1433 cm^{-1} (Figure 3). The 1545 cm^{-1} trough most likely arises from an amide II change of peptide backbone that is deeply buried and thus not susceptible to H/D exchange. Such a site could occur in the hydrophobic inner core of the protein complex, possibly toward the interior of dIII or in the membrane-spanning dII component. The NADP(H)-binding site is probably located some 30 Å from dII.[9] Thus, if NAD(P)H-binding leads to the conformational changes in protein backbone in the hydrophobic membrane-spanning region, the conformational change associated with the 1545 cm^{-1} band must occur over a considerable distance. Energy coupling between the redox reaction at the dI/dIII interface and proton translocation through dII is mediated by processes occurring at the NADP(H)-binding site in dIII.[40−42] It is tempting, therefore, to suggest that the changes at 1545 cm^{-1} caused by the binding of NADP(H) are a reflection of events on the energy coupling pathway.

Bands Due to Specific Amino Acids. Other features of the NAD(P)(H)-binding spectra might correspond to conformational changes in amino acid side chains during nucleotide binding to the enzyme. Several small but reproducible bands are evident in the spectra at frequencies for which amino acid side chains have characteristic absorbance bands. However, at this initial stage in our work, only possibilities may be suggested for further study. It was argued above that the band at 1705−1707 cm^{-1} in the NADP(H)-induced spectra (Figure 2) is unlikely to derive from the amide carbonyl group of the (dihydro)nicotinamide. This region of the spectrum is slightly below the range reported for bands of the C═O stretch of protonated carboxylic acid groups having a single hydrogen bond and is rather high for an amide I band. However, C═O stretch bands of protonated carboxylic acids having two hydrogen bonds have been reported in the 1703−1710 cm^{-1} range,[43] and a band in this range was previously suggested to originate from a protonated carboxylic acid group.[44] Thus, if not arising from a nucleotide or amide I change, the 1705−7 cm^{-1} peak could result from the protonated side chain of an Asp or Glu residue with two hydrogen bonds. The peak might be linked to the 1396−1398 cm^{-1} trough that possibly arises from the loss of the υ_s mode of the deprotonated form of the same carboxylic group (the associated υ_{as} COO^- band will be expected around 1570 cm^{-1} but would be masked by amide II changes). Considering this in relation to crystallographic data prompts the speculation that NADP(H) binding results in the protonation of the invariant βAsp392 in dIII. Substitution of this residue has profound effects on the activity of transhydrogenase.[38,45,46] In crystal structures of dIII,[6−8] the equivalent of βAsp392 makes contact with the nucleotide pyrophosphate group and is buried by loop E (see Figure 1), a secondary-structure element that is important in preventing release of bound NADP(H) into the solvent in the occluded state.[10] The pK_a of this residue is approximately 9.8 in the occluded state[2,47] and is suggested to decrease as loop E is raised during formation of the open state of the enzyme.[2] Thus, when NADP(H) binds to the intact transhydrogenase in the experiments reported here, and the enzyme open state equilibrates with the occluded state, βAsp392 is predicted to undergo protonation during closure of loop E.

The changes induced by H/D exchange in the amide I region of both the NAD(P)H-induced difference spectra are rather larger than expected if the bands arise solely from amide I shifts. The nucleotides themselves will have bands that shift markedly in this region (Figure 4). Furthermore, amino acid residues such as arginine and asparagine have two major bands within this envelope, and these, if shifted, could contribute to the spectral changes observed.

In summary, ligand-induced IR difference spectra of transhydrogenase can be generated at sufficient signal/noise to reveal aspects of binding of not only the nucleotides themselves but also responses of specific parts of the protein structure itself. The data reported here provide a first indication of the types of information that may be accessible. Testing and further refinement of possible assignments can be achieved through use of isotopically labelled versions of substrates with wild-type protein and with mutants in which specific amino acid residues have been modified.

Materials and Methods

Protein Purification. In previous work, *E. coli* transhydrogenase with a 6-His tag at the N-terminus of the α-subunit was expressed, under the control of its own promoter, from either a pUC-based plasmid (pNHis) or a pGEM-based plasmid (pNH).[48] Using equivalent procedures, we have constructed a plasmid (pNIC4) which encodes an identical protein but is expressed under the control of the strong T7 promoter in a pET-based vector. The starting construct (pSA2), which was generously provided by Dr. P. D. Bragg[49] and which encodes the complete *E. coli* transhydrogenase gene, was digested with *Hin*dIII and *Sph*I. The resulting 1.8 kb fragment was isolated, and a 1.1 kb segment of this was amplified by PCR using primers, 5′-$T_3ATA_2CATATG$-$(CAT)_5CACG_2TCGA_2T_2G_2CATAC_2A_2GAGA_2CG_2$-3′ and 5′-$TCACGC_2$-$GCGA_2TCAC_2ACATC$-3′. The product has an *Nde*I site upstream from DNA encoding the N-terminal region of the transhydrogenase α subunit, modified as in ref 48 to include the His tag, and it extends downstream of an *Eco*RV site. After DNA sequencing to ensure there were no polymerase errors, the 1.1 kb product was digested with *Nde*I and *Eco*RV and the resulting 0.8 kb fragment was purified. In parallel, the pSA2 construct was digested with *Xho*I and *Eco*RV, and pET21a (from Novogen) was digested with *Nde*I and *Xho*I, and the 2.2 and 5.4 kb fragments, respectively, were isolated. The 0.8, 2.2, and 5.4 kb fragments were ligated to reconstruct a His-tagged transhydrogenase gene in the pET vector, and this was designated pNIC4.

An *E. coli* strain, based on BL21(DE3)[50] but lacking the chromosomal transhydrogenase gene, was constructed as a host for pNIC4.

(40) Yamaguchi, M.; Stout, C. D.; Hatefi, Y. *J. Biol. Chem.* **2002**, *277*, 33670−33675.
(41) Althage, M.; Bizouarn, T.; Rydström, J. *Biochemisry* **2001**, *40*, 9968−9976.
(42) Whitehead, S. J.; Rossington, K. E.; Hafiz, A.; Cotton, N. P. J.; Jackson, J. B. *FEBS Lett.* **2005**, *579*, 2863−2867.
(43) Nie, B.; Stutzman, J.; Xie, A. *Biophys. J.* **2005**, *88*, 2833−2847.
(44) Noguchi, T.; Sugiura, M. *Biochemisty* **2003**, *42*, 6035−6042.
(45) Meuller, J.; Hu, X.; Bunthof, C.; Olausson, T.; Rydström, J. *Biochim. Biophys. Acta* **1996**, *1273*, 191−194.
(46) Fjellström, O.; Axelsson, M.; Bizouarn, T.; Hu, X.; Johansson, C.; Meuller, J.; Rydström, J. *J. Biol. Chem.* **1999**, *274*, 6350−6359.
(47) Pedersen, A.; Johansson, T.; Rydström, J.; Karlsson, B. G. *Biochim. Biophys. Acta* **2005**, *1707*, 254−258.
(48) Meuller, J.; Rydström, J. *J. Biol. Chem.* **1999**, *274*, 19072−19080.
(49) Ahmad, S.; Glavas, N. A.; Bragg, P. D. *Eur. J. Biochem.* **1992**, *207*, 733−739.
(50) Studier, F. W.; Moffatt, B. A. *J. Mol. Biol.* **1986**, *189*, 113−130.

Plasmid pDC21 (also supplied by Dr Bragg[4]) was prepared from *E. coli* JM110 (*dam*$^-$ *dcm*$^-$) to prevent DNA methylation. It was digested with *Xho*I and *Bcl*I, which excised a 1840-base fragment encoding the last 298 amino acids of the *E. coli* transhydrogenase α-subunit and the first 310 amino acids of the *β*-subunit. The removed sequences included all of the transhydrogenase membrane domain, dII. The fragment was replaced by a cassette containing the kanamycin-resistance gene (Km^r) from pUC4K.[51] As the existing restriction sites in pUC4K were unsuitable, a 1.2 kb fragment containing Km^r was amplified by PCR, using the primers (5′-AGTGAG$_3$ATC$_2$ACG$_2$T$_2$GATGAG-3′) and (5′-G$_2$A$_3$CAGCTATGATCATGAT$_2$ACG-3′). The PCR product was digested with *Bam*HI and *Sal*I and ligated into the *Xho*I/*Bcl*I-digested pDC21 to produce pPQ3. A linear 2.2 kb fragment of pPQ3, comprising Km^r flanked by 600 bases of *E. coli pntA* and 460 bp of *E. coli pntB*, was amplified by PCR, using the primers (5′-AT$_2$G$_2$CATAC$_2$A$_2$GAGA$_2$-CG$_2$-3′) and (5′-CAGAGCT$_3$CAG$_2$AT$_2$GCATC$_2$ACG-3′). The fragment was electroporated into *E. coli* RK4353[52] carrying pKD46,[53] and the cells were plated out at 37 °C in the presence of kanamycin. Plasmid pKD46 carries the Red recombination system, allowing efficient uptake and chromosomal integration of linear DNA,[54] and also confers resistance to ampicillin. The plasmid cannot replicate at 37 °C, and colonies were tested for resistance to kanamycin, resulting from recombination of the Km^r cassette into the bacterial chromosome, together with sensitivity to ampicillin, indicating the loss of pKD46. One ampicillin-sensitive, kanamycin-resistant colony was found, and PCR amplification across the *pnt* operon, along with restriction mapping, verified that only the interrupted *pnt* genes were present, indicating that the desired homologous recombination had occurred. The interrupted *pnt* genes were transferred into *E. coli* BL21(DE3) by P1 phage transduction. Candidate kanamycin-resistant colonies were screened by PCR for the presence of the T7 RNA polymerase gene (integrated into the chromosome of BL21(DE3)) and the interrupted *pnt* genes, together with the loss of the wild-type *pnt* genes. They were also checked for the absence of plasmids. The deletion strain was designated BL21(DE3) Δ*pnt*. Membranes prepared from this strain had no detectable transhydrogenase activity (data not shown).

When required, BL21(DE3) Δ*pnt* was transformed with pNIC4. Single colonies of transformants were taken from LB plates containing kanamycin (50 μg mL^{-1}) and ampicillin (100 μg mL^{-1}) into liquid LB medium also containing the two antibiotics. Cells were induced with 0.25 mM isopropyl thiogalactoside. The harvested cells were washed in TED buffer (50 mM Tris-HCl, pH 8.0, 1 mM EDTA, 1 mM dithiothreitol) and stored at −20 °C. Membranes were prepared in TED buffer, as described,[31,55] resuspended in 15 mM sodium phosphate, pH 7.5, 50% glycerol, and stored at −20 °C.

Transhydrogenase was solubilized and purified (at 4 °C) by a modification of procedures described.[46,56] Thawed membranes were resuspended to a protein concentration of 2 mg mL^{-1} in 25 mM sodium cholate, 25 mM sodium deoxycholate, 1 M KCl, 0.5 mM 4-(2-aminoethyl)-benzenesulfonylfluoride HCl, 5 mM *β*-mercaptoethanol with one EDTA-free protease inhibitor tablet (Roche) in a 40 mL volume. The suspension was stirred for 20 min at 4 °C and centrifuged at 100 000 *g* for 45 min, and the supernatant was passed through a 0.45 μm filter. The filtered supernatant was incubated with NiNTA Superflow (6 mL bed volume, Qiagen) that had been pre-equilibrated with 30 mM sodium phosphate, pH 7.5, 7 mM imidazole, 0.5 M NaCl, 0.1% Brij35, 0.1% Thesit, 5 mM *β*-mercaptoethanol and loaded into a glass column, diameter 16 mm. The column was washed with the equilibration buffer (1 mL min^{-1}) until the absorbance at 280 nm fell to a minimum. It was washed again with 20 mM Tris-HCl, pH 8.0, 30 mM imidazole, 0.7 M NaCl, 0.1% Brij35, 0.1% Thesit, 5 mM *β*-mercaptoethanol, again until the absorbance at 280 nm fell to a minimum and the transhydrogenase was then eluted in 20 mM Tris-HCl, pH 8.0, 150 mM imidazole, 0.1 M NaCl, 0.1% Brij35, 0.1% Thesit, 5 mM *β*-mercaptoethanol. The protein, assayed by the bicinchoninic acid procedure,[57] was adjudged to be >90% pure on SDS-PAGE and had a specific activity (determined as in ref 24) of typically 5−7 μmol mg^{-1} protein min^{-1}. The purified protein solution (10 mL) was diluted at 4 °C with a similar volume of 30 mM sodium phosphate buffer, pH 7.5, 1 mM dithiothreitol, containing 0.03% dodecyl maltoside and centrifuged through a 100k Vivaspin filter to reduce the volume to approximately 2 mL. The concentrated protein was again diluted to 20 mL with the phosphate/dithiothreitol/dodecyl maltoside buffer and recentrifuged. This washing step was repeated twice.

Preparation of "ATR-Ready" Protein. Detergent depletion of the transhydrogenase preparation was required in order to produce an "ATR-ready" sample capable of forming a stable film on the surface of the silicon ATR prism. The procedure is basically similar to that described in ref 22. A sample of the protein solution prepared as described above (0.2 mL, approximately 200 μg protein) was diluted into 3 mL of 10 mM potassium phosphate buffer at pH 7.5 containing 0.005% w/v sodium cholate and 0.005% w/v octylglucoside. The protein was pelleted by centrifugation at 200 000 *g* for 60 min. The pellet was re-suspended in the same buffer but without detergent and re-pelleted by centrifugation at 150,000 *g* for 30 min. The washing step with detergent-free buffer was repeated 3 times. The resulting pellet was resuspended in 3 mL of 1 mM potassium phosphate at pH 7.5, and the material was again centrifuged. The final pellet was resuspended in 50 μL of distilled water (ATR-ready sample) and used immediately or stored at −80 °C. A 1.2 μL aliquot of an ATR-ready sample (approximately 4−5 μg protein) was diluted with 2 μL of distilled water and placed on the surface of an ATR prism. After drying in a gentle stream of N_2, the sample was rehydrated with perfusion buffer (100 mM potassium phosphate, 2 mM $MgCl_2$, pH 7.2). Before measuring nucleotide-induced difference spectra, the film was perfused with the same buffer at a flow rate of 0.5 mL/min for 60 min to remove residual dodecyl maltoside which had remained bound to the protein. For measurement in D_2O media, purified transhydrogenase was made as described above but the subsequent procedures for preparing the "ATR-ready" sample were all performed in D_2O media assuming pD = $pH_{reading}$ + 0.4.[58] Representative absolute ATR-FTIR absorption spectra of protein films in H_2O and D_2O media are shown in the Supporting Information. The extent of H/D exchange was estimated to be >90% by the method described in ref 59.

Nucleotide-Induced ATR-FTIR Measurements. ATR-FTIR spectra of the protein film were recorded at 20 °C and 4 cm^{-1} resolution with a Bruker ISF 66/S spectrometer, fitted with a liquid-nitrogen-cooled MCT-A detector. Nucleotides ($NADP^+$, NADPH, NAD^+, and NADP) were dissolved in the perfusion buffer (H_2O or D_2O media) at indicated concentrations. A background spectrum of the film (an average of 500 interferograms) was first recorded during perfusion with buffer in the absence of nucleotides. The buffer was then switched to one containing nucleotide, and after a 5-min delay for equilibration, a ligated *minus* unligated difference spectrum was recorded (an average of 500 interferograms). Then, a new background was taken, buffer was switched back to one without nucleotide, and after a 6-min delay, an equivalent unligated *minus* ligated difference spectrum was recorded. The cycling procedure was repeated 10−60 times, and the difference spectra were calculated as averages of ligated *minus* unligated and inverted unligated *minus* ligated spectra. The flow rate was maintained

(51) Vieira, J.; Messing, J. *Gene* **2005**, *19*, 259−268.
(52) Stewart, V.; MacGregor, C. H. *J. Bacteriol.* **1982**, *151*, 788−799.
(53) Datsenko, K. A.; Wanner, B. *Proc. Natl. Acad. Sci. U.S.A.* **2005**, *97*, 6640−6645.
(54) Murphy, K. C. *J. Bacteriol.* **1998**, *180*, 2063−2071.
(55) Tong, R. C. W.; Glavas, N. A.; Bragg, P. D. *Biochim. Biophys. Acta* **1991**, *1080*, 19−28.
(56) Hu, X.; Zhang, J.-W.; Persson, A.; Rydström, J. *Biochim. Biophys. Acta* **1995**, *1229*, 64−72.
(57) Smith, P. K.; Krohn, R. I.; Hermanson, G. T.; Mallia, A. K.; Gartner, F. H.; Provenzano, M. D.; Fujimoto, E. K.; Goeke, N. M.; Olson, B. J.; Klenk, D. C. *Anal. Biochem.* **1985**, *150*, 76−85.
(58) Glasoe, P. K.; Long, F. A. *J. Phys. Chem.* **1960**, *64*, 188−190.
(59) Rath, P.; DeGrip, W. J.; Rothschild, K. J. *Biophys. J.* **1998**, *74*, 192−198.

at 1 mL/min, and all spectra were recorded at room temperature. All frequencies quoted have an accuracy of ± 1 cm^{-1}.

ATR-FTIR Spectra of Substrates and Model Compounds. Absolute ATR-FTIR spectra of $NADP^+$, NADPH, NAD^+, and NADH substrates (40 mM) were measured in perfusion buffer in both H_2O and D_2O media. Spectra of a range of related model materials (ribose, adenosine, ADP, ADP-ribose, and reduced and oxidized forms of nicotinamide mononucleotide) were also recorded in H_2O or D_2O media to aid assignment of principal bands to specific parts of the nicotinamide dinucleotides. In all cases a 10-μL aliquot of sample solution was placed on the ATR prism, and its absolute spectrum was recorded (an average of 2000−3000 interferograms). An equivalent spectrum of buffer alone was recorded separately and subtracted from that of the test solution. In the case of adenine, a grain of reagent was dissolved in ethanol, and an aliquot was deposited on the ATR prism. The absolute absorption spectrum of ethanol was subtracted from the spectrum shown. Its amplitude was rescaled in Figure 5 to be comparable to other model data.

Acknowledgment. We thank the Biotechnology and Biological Sciences Research Council (BBS/B/01456 to J.B.J. and BB/C51715X/1 to P.R.R.) for financial support and Mr. Santiago Garcia (UCL) for expert technical support.

Supporting Information Available: Absolute ATR-FTIR spectra of transhydrogenase films in H_2O and D_2O media, and difference spectra induced by different concentration of NADPH are presented in the Supporting Information. This material is available free of charge via the Internet at http://pubs.acs.org.

JA0556272